Empirical Quantification and Modeling of Muscle Deformation: Toward Ultrasound-Driven Assistive Device Control*

Laura A. Hallock[1], Akira Kato[2], and Ruzena Bajcsy[1]

***Abstract*— Surface electromyography is currently the sensing modality of choice for control of biosignal-driven prostheses and exoskeletons; however, the sensor's noisy and aggregate nature inhibits collection of distinguishable signal streams to robustly manipulate multiple device degrees of freedom (DoF). We here explore 2D B-mode ultrasound as an alternative source of muscle activation data (namely, muscle deformation) that can be more precisely localized, allowing for the theoretical collection of multiple naturally-varying signals that could be used to control high-DoF assistive devices.**

We here present a proof-of-concept study showing *a)* the observability of muscle deformation via ultrasound, and *b)* novel descriptions of the spatially-varying nature of the signal. These analyses are accomplished through the study of nine volumetric scans of the biceps brachii under varied elbow angle and loading conditions, collected and spatially localized using an ultrasound scanner and motion capture. We here establish the feasibility of measuring several force-associated deformation signals (including muscle cross-sectional area and thickness) via real-time ultrasound scanning and quantify the spatial variation of these signals. Additionally, we propose future applications for both our signal characterizations and the generated muscle volume data set, including better design of assistive device sensor locations and validation of existing muscle deformation models.[†]

I. Introduction

Although there exist a wide variety of mechanically-sophisticated upper-limb prostheses and exoskeletons, none are able to truly replicate the functionality of the intact human arm in terms of movement precision and functional flexibility. This is largely because controlling such a device requires the robust manipulation of a prohibitively large number of control signals; a fully biomimetic arm exoskeleton, for example, would need to not only actuate the 34 kinematic degrees of freedom (DoF) of the arm and hand, but modulate the torque applied at each joint to allow for varying levels of output force. Indeed, the true degrees of freedom of the human arm are better described in terms of its actuators — more than 30 muscle groups, which can be actuated synergistically or independently to modulate both kinematic configuration and joint stiffness, each of which consists of hundreds of thousands of muscle fibers and billions of sarcomeres.

*This work was supported by the NSF National Robotics Initiative (award no. 81774), Siemens Healthcare (85993), and the NSF Graduate Research Fellowship Program.

[1]Laura Hallock and Ruzena Bajcsy are with the Department of Electrical Engineering and Computer Sciences, University of California, Berkeley, Berkeley, CA 94720, USA {lhallock, bajcsy}@eecs.berkeley.edu

[2]Akira Kato is with the Graduate School of Creative Science and Engineering, Waseda University, Shinjuku, Tokyo 169-0072, Japan k-ing@fuji.waseda.jp

[†]A visual summary of the work described can be found in the accompanying video abstract.

Requiring an assistive device user to learn to reliably manipulate even a few disjoint control signals, often under diminished physical capacity, is largely infeasible. Instead, device designers rely on the use of biological control signals — most commonly, surface electromyography, or sEMG — to measure muscle activation that users are already practiced at modulating. This signal is then integrated into the device control scheme in a manner that (ideally) allows for more intuitive control.

At the same time, sEMG — a measure of the electrical signals sent by the neurological system to initiate contraction, which are then amplified to observable levels within the muscle — provides an aggregate, noisy signal that varies greatly with even small shifts in sensor placement. As a result, the vast majority of sEMG-driven devices allow for the control of only a single DoF, using the signal differential between agonist and antagonist muscles to modulate the configuration of a single joint or closure of a grasp [1] or relying entirely on deep learning classification techniques [2].

Due to its aggregate nature and lack of robustness, sEMG cannot be used to acquire the kind of localized muscle activation data necessary to allow for intuitive control of high-DoF assistive devices. While its use is all but ubiquitous, sEMG is not the only modality capable of sensing muscle state — nor is the electrical signal it measures the only measure of muscle activation. In this paper, we examine *muscle deformation* as an alternative measure of muscle activation and explore the feasibility of measuring this deformation via *2D brightness mode (B-mode) ultrasound*.

Muscle deformation is known to be observable and correlated with output force. In general, active muscle contraction causes the constituent fibers to shorten, and the muscle expands in other dimensions such that a constant volume is maintained, stretching the surrounding fascia and aponeuroses both parallel and perpendicular to the line of action [3]. However, similar deformation also occurs under changes in kinematic configuration, as muscles are passively stretched to accommodate new distances between their attachment points and deformed by interactions with the surrounding tissues. A framework that uses muscle deformation changes as a measure of force output must therefore account for these configuration-associated deformation changes. However, the manner in which these deformations interact remains poorly understood, due to both the difficulty of formulating and appropriately fitting high-DoF deformation models and the lack of data that would allow for model validation.

In this study, we seek to explicitly measure and characterize both force- and configuration-associated muscle deformation by examining volumetric changes in the biceps brachii

across multiple elbow flexion angles and loading conditions. In order to extract these volumetric values under each condition, we collect a dense data set of B-mode ultrasound scans along the anterior surface of the arm, each of which is spatially localized via calibration of the marker-tagged ultrasound probe with an active motion capture system. These scans are then used to build a 3D intensity map within which muscle fascia can be readily observed, thus allowing for segmentation of the complete biceps brachii volume. The resulting volumetric data are then examined spatially along the length of the arm and in relation to scans under different kinematic and loading conditions as a preliminary study of the two types of deformation and the differences between them.

This paper presents the following novel contributions:

- a *set of volumetric data* of the biceps brachii and other elbow flexors under factorial elbow flexion angles and loading conditions, to allow for the first-ever separable analysis of force- and configuration-associated muscle deformation of the same subject; and
- a *proof-of-concept study* confirming the ready observation of both force- and configuration-associated deformation of the biceps brachii and a characterization of this deformation along the length of the arm.

The two contributions above permit us to conjecture promising locations from which to extract an elbow flexion control signal from a single time-varying ultrasound scan, an observation with ready applications in the prosthesis design community. Furthermore, the localized nature of the ultrasound signal means that such scans could be used to observe multiple muscle groups simultaneously and individually — a step toward the development of control schemes for high-DoF biomimetic assistive devices.

II. Related Work

While the study of muscle deformation spans a number of disciplines, from computer animation to biophysics, there exist few macro-scale models relevant to assistive device control, and fewer still are (even cursorily) validated with experimental data. Within the field of computer graphics, a number of algorithms exist to generate plausible muscle deformations given a virtual model's kinematic configuration, dynamics, and/or skin surface deformation [4]–[7], but these algorithms are generally evaluated on their output's visual appeal rather than a physiological or data-driven error metric. Although some such models are rooted in biomechanical data and are intended for real-world medical applications [7], they largely ignore muscles' fundamental nature as actuators, instead treating them as passive elements whose deformation is purely a function of configuration and applied external force. Lastly, most of these models rely on finite element analysis, which makes them too computationally intensive for direct application to a real-time control scheme.

At the other end of the muscle deformation modeling spectrum are micro- and mezzo-scale analyses of (one to a few) individual muscle fibers [8], [9]. While these models offer significant insight into the biological sources of deformation, they are not readily extensible to macro-scale analysis. Indeed, there is significant evidence not only that fibers behave quite differently in vivo and in isolation, but that passive tissues like tendons and aponeuroses significantly impact the deformation behavior of the muscle-tendon unit when modeled at this level of detail [10]. This evidence makes it difficult or impossible to conjecture how deformations scale across model resolution.

Despite this dearth of models, deformation has been employed as an assistive device control signal, using noninvasive sensing modalities like force myography (FMG) [11] and tactile myography (TMG) [12] to measure shape and force changes at the surface of the skin. These methods show great promise in augmenting existing sEMG technology but cannot yield insight into the complex deformation relationships between deep and surface muscles that characterize many joints' actuation. Elbow joint flexion, for example, is generated not only by the biceps brachii and brachioradialis, both surface muscles, but also by the (deep) brachialis.

While commercial ultrasound-driven assistive devices are not yet available, diverse studies have demonstrated the use of B-mode ultrasound to classify hand motions [13] and measure a wide variety of muscle architectural parameters, including muscle thickness, pennation angle, and fascicle length [14]. A number of studies have specifically targeted muscle thickness, both as a feasible signal for prosthesis control [15] and as a measure of muscle activation (as correlated with EMG) [16], [17] and fatigue [18]. Additionally, wearable 1D amplitude mode (A-mode) ultrasonic sensors — which could potentially be applied to acquire a single muscle thickness measurement — have been used to continually monitor the mechanical properties of plantar soft tissue in diabetic patients [19] and knee torque [20] and are much closer to commercial integration with assistive devices than 2D B-mode scanners.

B-mode ultrasound — and, as the technology evolves, A-mode ultrasound — is thus a promising sensing modality for the acquisition of muscle deformation data, both statically (during the collection of morphological data) and as a source of real-time control signals to drive assistive devices. In this study, we examine the use of ultrasound in each manner, first gathering static volumetric data of the muscles about the elbow under multiple conditions, then examining the spatial distribution of muscle deformation along the arm to draw conjectures about promising locations from which to measure an assistive device control signal. In performing these two analyses, we hope to *a)* augment existing studies of ultrasound-measured muscle deformation by providing a more complete understanding of the signals observed, and *b)* inform new muscle deformation studies, both by characterizing where deformation associated with varying kinematic configuration and load conditions is most observable and by providing a data set that allows for further domain-specific study of the topic.

III. Volumetric Data Collection

Volumetric muscle data were collected from the elbow flexors of a single subject under three kinematic configurations (i.e., elbow angles) and three loading conditions in a full factorial manner, with factors and levels as listed in Table I. The deformation measurements listed were then

TABLE I

VOLUMETRIC DATA COLLECTION CONDITIONS & DEFORMATION ANALYSES

Manipulated Factors		Levels*	**Deformation Measurements**		**Analyses**
θ	elbow flexion angle	*0°*, 30°, 60°, 90°	$\text{CSA}_{\theta,LC}(x)$	muscle cross-sectional area	variation in x
			$\text{T}_{\theta,LC}(x)$	muscle thickness	maximum value
LC	elbow load condition	fully supported (FS),	$\text{E}_{\theta,LC}(x)$	eccentricity of muscle cross-section	x loc. of maximum value
		gravity compensation (GC),		(at dist. x from muscle origin)	quadratic regression in x
		under load of 227g (LF),			
		under load of 727g (MF),	$\Delta\text{CSA}_{\theta,LC}(x)$	$\text{CSA}_{\theta,LC}(x) - \text{CSA}_{\theta,FS}(x)$	
		under load of 954g (HF)	$\Delta\text{T}_{\theta,LC}(x)$	$\text{T}_{\theta,LC}(x) - \text{T}_{\theta,FS}(x)$	

**Italicized values denote conditions for which raw ultrasound data were collected but for which volumetric data reconstruction has not yet been completed; these scans will be used in future analysis and validation of the results included here. Note that "fully supported" (FS) trials occurred while the arm was fully supported by the experimental jig (i.e., to measure "pure" kinematic deformation), while the "gravity compensation" (GC) trials occurred while the arm was unsupported but unloaded (i.e., the elbow flexors performed gravity compensation for the arm's mass, but nothing more).*

extracted from the segmented biceps brachii of each of the nine resulting scans and analyzed along the axis of the humerus (hereafter denoted x). Selected results of the listed analyses are discussed in Section IV.

We here provide a detailed description of the experimental procedures used to collect the raw ultrasound data, reconstruct the spatial location of each ultrasound scan, extract the relevant muscle volumes and bone surfaces, and process the volumes into the deformation measurements used in our analyses. While we have here chosen a set of exploratory analyses that are relevant to the choice and localization of control signals for assistive devices, the volumetric data we reconstruct admits a wide range of biometric analyses and has been made available on the Human Assistive Robotic Technologies Lab website (`hart.berkeley.edu`) to permit further exploration.

A. Subject Biometric Data & Consent

Data were collected from the right arm of a male subject, age 25, of mass 55kg and height 1.6m. Because the manual extraction of muscle volumes presents a prohibitively time-consuming bottleneck, as described in Section III-C, only data from this single subject are presented here. Data were collected from the right arms of two additional subjects (female, age 24, mass 70kg, height 1.8m and male, age 21, mass 66kg, height 1.6m) for future analysis and publication. All subjects were healthy and right-handed.

The study protocol was approved by the University of California Institutional Review Board for human protection and privacy, under Protocol ID 2016-01-8261. Each subject was first informed of the experimental procedure and written informed consent was obtained.

B. Data Collection

During data collection, the test subject lay supine and relaxed, with legs comfortably extended and right arm extended laterally from the body at a 90° shoulder abduction angle. The forearm was fully supinated, with the upper arm supported at the distal end of the humerus, as shown in Figure 1. Scans were then collected with the subject's elbow held statically at each of the three angle values listed

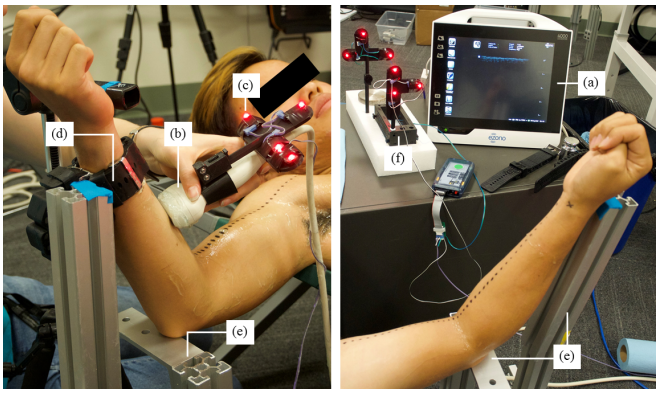

Fig. 1. Experimental setup for the collection of full-arm upper-limb morphology data under multiple elbow angles and loading conditions, enabling a factorial study of the sources of muscle deformation (shown here at a 60° angle of elbow flexion under HF (*left*) and FS (*right*) loading conditions). Setup includes ultrasound scanner (a) and probe (b) (with attached active motion capture markers (c) used for spatial tracking); weight bands (d) used to load the elbow flexors (during LF and HF trials); mechanical jig (e) used to support the elbow (during all trials, *left*) and the forearm (during FS trials, *right*); and the phantom devices (f) required to calibrate the coordinate transformation between the motion capture world frame and the measured ultrasound scans.

in Table I (as measured from from full extension) under three separate loading conditions (fully supported by a jig at the wrist and unsupported while lifting wrist weights of comparatively low and high mass), for a total of nine trials. Angle conditions were selected to allow for both observable kinematic-associated muscle deformation and free manipulation of the ultrasound probe around the elbow joint (the latter of which precluded scans at larger elbow flexion angles). Similarly, loading masses were selected to allow for observable force-associated muscle deformation while not being so heavy that subjects were unable to remain still during the (several minute) duration of the scan. During unsupported weight-bearing trials, subjects were asked to maintain contact between a designated point on the anterior surface of the wrist and a guide bar in order to maintain constant elbow flexion angles both within and between trials. Loading weights were attached at the wrist to avoid the

confounding activation of wrist and finger flexors that would occur if weights were held in the hand.

During each trial, ultrasound images were collected using a portable commercial ultrasound scanner (eZono 4000, eZono AG, Jena, Germany) equipped with a 3-12MHz linear transducer (L3-12 NGS, eZono AG, Jena, Germany). The machine was configured to collect B-mode data at a depth of 4cm, with a 3.8cm transducer footprint.

To collect full volumetric data of the anterior surface of the arm, the ultrasound probe was held perpendicular to the subject's skin and swept by a practiced operator along the arm's surface, using the minimum pressure necessary to maintain probe contact in order to deform the tissue as little as possible. To scan the full anterior surface of the arm (from medial to lateral edges) required multiple parallel sweeps of the probe; to ensure that scans were sufficiently evenly distributed in space, the subject's arm was marked in 1cm increments using a non-toxic marker, and the operator maintained a metronome-guided constant rate of approximately 80cm/min when sweeping proximally-to-distally along the arm, deviating as necessary near the shoulder and elbow joints to acquire sufficient numbers of scans. (Note that the volumetric reconstruction of these scans used here does not impose specific requirements on the spatial distribution of data, so this process need not be completely rigorous and simply improves signal quality.)

To permit volumetric reconstruction of the ultrasound data, the spatial location of the probe was tracked from a set of four optical markers using a PhaseSpace active motion capture system (PhaseSpace Inc., San Leandro, CA, USA). Prior to data collection, the transformation between the ultrasound probe location and the measured image was calculated (both spatially and temporally) using the open-source PLUS calibration toolkit [21], with a reported probe calibration error of 1.6mm. During data collection, data were streamed to an external computer at a rate of 30fps through an OpenIGTLink server [22] and later reconstructed using the volume reconstruction application provided by the PLUS toolkit.

The full experimental setup is shown in Figure 1, and representative volumetric data can be seen in Figure 2 as the spatial intensity map from which volumes were manually segmented.

C. Muscle Volume Extraction

A complete study of muscle deformation about the elbow would require characterization of all muscles that actuate the joint, including flexors and extensors, as well as the muscles of the surrounding joints that contact and collide with those above. While this study includes preliminary segmentation results of all elbow flexors (biceps brachii, brachialis, and brachioradialis), we report primarily on the observed deformation of the biceps brachii, which can be most cleanly observed in all nine scans examined and — as a surface muscle — is a natural target for eventual use in assistive device control signals. While the brachialis muscle is also known to exert significant force during elbow flexion, the fact that its belly is largely centered over the elbow joint itself makes deformation difficult to observe and characterize (unlike the biceps brachii, whose mass is concentrated along the upper arm). The brachioradialis was not prioritized for scanning, as it primarily impacts elbow flexion when the wrist is pronated, and is not always completely visible within the frame of our scans.

For initial segmentation, we selected the scan collected at a 30° elbow flexion angle while fully supported, as this condition represents a natural baseline for all subsequent conditions that increase angle and loading. Muscle volumes for the biceps brachii, brachialis, and brachioradialis were observed and manually annotated in the axial, coronal, and sagittal planes of the scan using ITK-SNAP [23], as were the anterior surfaces of the humerus, ulna, and radius (in order to establish the locations of both muscle attachment points and the elbow joint itself).

The full manual segmentation of this initial scan represents a bottleneck in the analysis process: it took two operators tens of hours to complete the full segmentation at the desired level of precision. To segment additional scans, a manual rigid transformation was performed in 3D Slicer [24] to align the segmentation of the initial scan with each of the remaining eight volumetric scans, such that the humerus of each scan perfectly overlapped. These segmentations were then manually modified in ITK-SNAP to include the new muscle deformation observed and any other necessary clean-up (a process that took several hours per scan rather than several days).

In addition to decreasing the required segmentation time, this process of modifying an existing segmentation instead of segmenting from scratch mitigated the chances of the human segmenter encountering areas of scan ambiguity (e.g., wide muscle fascia, bone shadow, poor signal quality around the elbow joint) and making different choices across scans, generating a deformation signal that could be erroneously attributed to configuration- or force-associated deformation. To further reduce the prevalence of these types of errors, all nine scans were manually aligned (again using humerus alignment as ground truth) and were simultaneously examined by the same segmenter, slice by slice, to ensure that segmentation ambiguities were resolved consistently across scans.

The final result of this segmentation process is a set of nine aligned upper-arm scans at the factorially-varying elbow flexion and loading conditions described above, as shown in Figure 2. These scans have been made available for public use and are here used to characterize observable muscle deformation signals.

D. Extraction of Deformation Signals

Because we ultimately hope to employ muscle deformation signals in assistive device control, we seek to observe signals that are *a)* well-correlated with the force output of the muscle, *b)* measurable from a single ultrasound data stream, and *c)* robust to variation in sensor location. With these characteristics in mind, we here extract the values of the following three signals (noted spatially on a representative scan in Figure 3) at each cross section along the length of the arm.

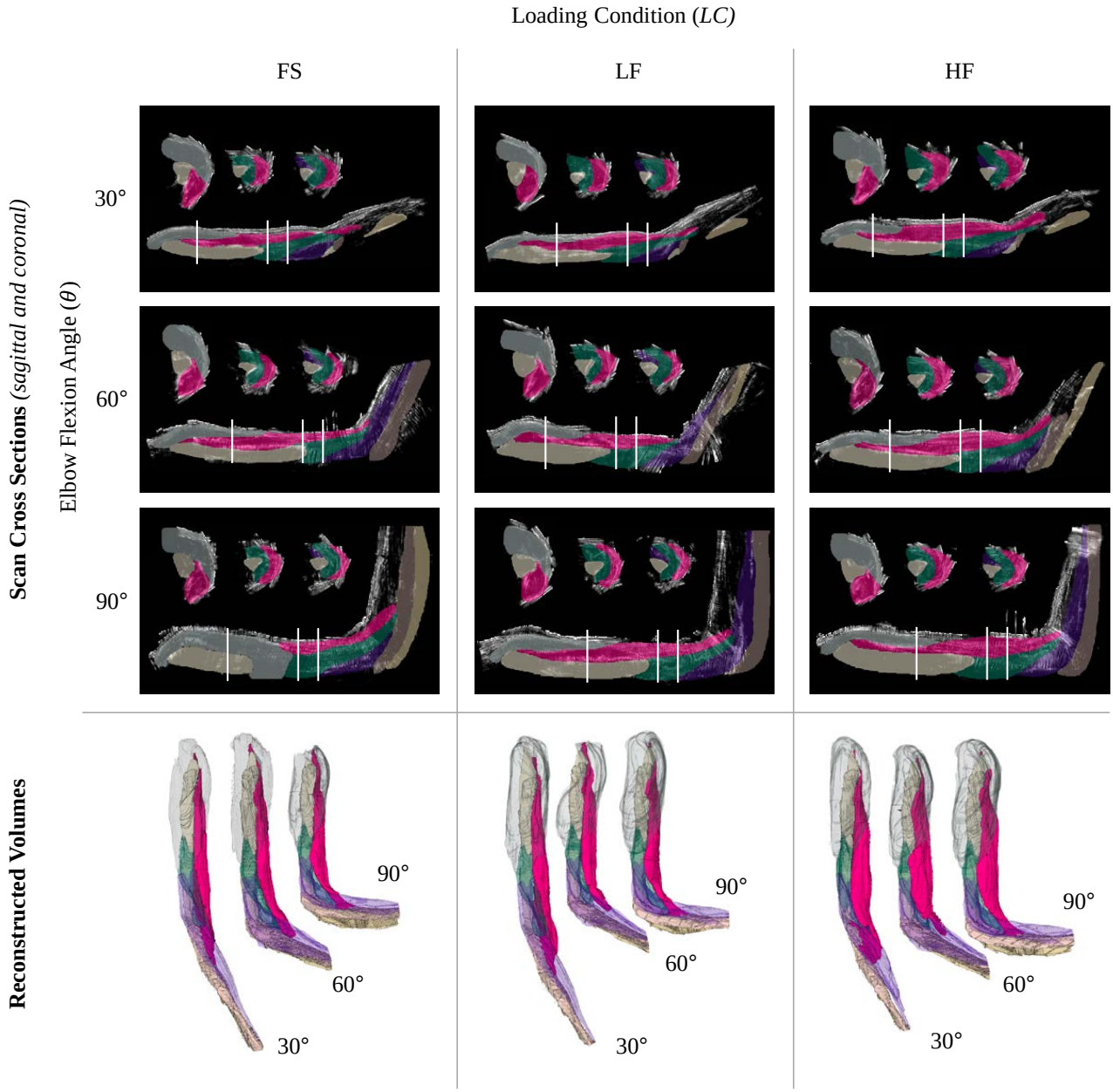

Fig. 2. Force-associated deformation of the (magenta) biceps brachii and surrounding muscles (turquoise brachialis, purple brachioradialis, and gray deltoid) under multiple loading conditions, as segmented from volumetric reconstruction of ultrasound data. Locations of the coronal cross-sectional scans shown are noted by lines transecting the associated sagittal scan in each inset. Volumetric changes across both kinematic configurations and loading conditions are readily observable, confirming the necessity of modeling both signal sources when employing muscle deformation as a device control signal.

1) Muscle cross-sectional area (CSA): A large body of research [25] suggests a complex but positively correlated relationship between force capability and CSA; we here explore whether changes in this CSA are also indicative of force output. We define CSA as the area of the muscle cross section sliced perpendicular to the length of the humerus.

2) Muscle thickness: Muscle thickness is a promising assistive device control signal, as there is strong evidence that it can be measured in real time from B-mode (and even A-mode) ultrasound data [15]. While it is not at all obvious how to define this value spatially across muscle cross sections — since defining it relative to any single axis along the humerus cannot accommodate the nonlinear deviation of the muscle along its length — we here define thickness as the mean thickness of the muscle measured from the anterior arm surface down toward the humerus within a 1cm window surrounding the centroid of the measured muscle cross section.

3) Eccentricity of muscle cross section: We here define the eccentricity of the muscle cross section as the condition number of the covariance matrix of each muscle cross section when treated as spatially-varying point data. Intuitively, the

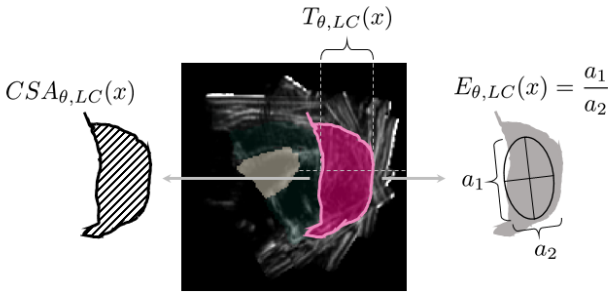

Fig. 3. Visualization of metrics used in spatial deformation analysis on a single representative coronal cross section. Cross-sectional area $\mathrm{CSA}_{\theta,LC}(x)$ was directly extracted from the segmented volumetric biceps volume, and thickness $\mathrm{T}_{\theta,LC}(x)$ was computed as the mean of the measure shown about a 1cm region surrounding the centroid of the computed area. Eccentricity $\mathrm{E}_{\theta,LC}(x)$ was computed as the major-to-minor-axis ratio of the best fit ellipse to the cross-sectional spatial data values in the least-squares sense. The data collected suggest that CSA changes are a robustly observable measure of muscle activation, and that thickness measurements, when combined with a model of eccentricity, could be used to estimate the CSA signal using cheaper A-mode ultrasound sensors.

condition number represents the ratio of the major to minor axes of the best-fit ellipse to the cross-sectional area and is thus a measure of muscle eccentricity along the length of the arm.

IV. Deformation Analysis

We here present preliminary observations on biceps brachii muscle deformation as measured by the three signals defined and extracted above. Note that there are no obvious a priori assumptions on how these values relate specifically to kinematic- or force-associated muscle deformation, or whether they can be used to discriminate between the two. To our knowledge, no literature exists on the topic, as the two types of deformation are typically studied in isolation.

A. Spatial Variation in Muscle CSA, Thickness, & Eccentricity

The top and middle plots of Figure 4 show raw CSA and thickness data for the biceps brachii under the fully-supported condition at all three angles examined, as well as the best-fit quadratic regressor for the data (in the least-squares sense), from the proximal extremum of the observable biceps volume to the location of the elbow (i.e., where the humerus meets the radius and the ulna).

The compression of the muscle with increased angle is observable in the width of the best-fit quadratic CSA functions: the model for the 30° condition is widest, and that of the 90° condition is narrowest. At the same time, while intuition might indicate that the location of maximum CSA and thickness value drifts from distal to proximal with increasing angle, we observe no such change under the angle conditions tested. Instead, the fitted quadratic functions consistently peak at a distance of 7.4cm (46%) from the proximal end of the muscle across all angle conditions (all within a range of 0.3cm), and no obvious deviation from this mean is observable under load.

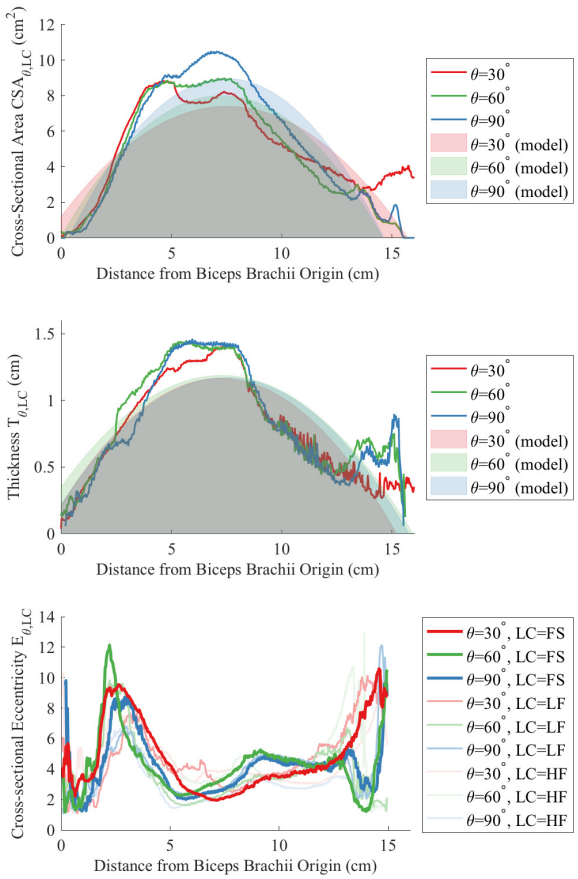

Fig. 4. Variation in cross-sectional area (*top*), thickness (*middle*), and eccentricity (*bottom*) along the length of the biceps brachii from shoulder to elbow, under multiple elbow flexion angles with the forearm fully supported. The location of maximum CSA/thickness (as measured from the corresponding quadratic regression models shown in overlay) was not shown to vary with angle, but the changes in width of the fitted CSA quadratics reflect the compression of the muscle as elbow flexion increases, a preliminary and intuitive insight that suggests that building low-dimensional predictive models of CSA change may be possible. The steep increase in eccentricity near the muscle's ends is reflected in the cross-sectional images shown in Figure 2, and the consistent shape of the eccentricity map across all tested conditions indicates that a spatial eccentricity map could be of use in developing a predictive model of muscle CSA from 1D thickness data.

The narrowing and flattening of the biceps near each end of the muscle is reflected in the eccentricity values shown in the final plot of Figure 4; this trend is also reflected qualitatively in the scan cross sections shown in Figure 2. While the raw eccentricity values do not present a straightforward understanding of spatial muscle deformation in isolation, they can be combined with muscle thickness — which can be measured with cheaper, simpler sensors like A-mode ultrasound — to generate an approximate model of muscle CSA. Once appropriately fitted to the data, such a model could form the basis of a control scheme driven by muscle thickness data, and the consistent overall shape of the eccentricity curve under all tested conditions indicates that the extraction of such a model may be possible.

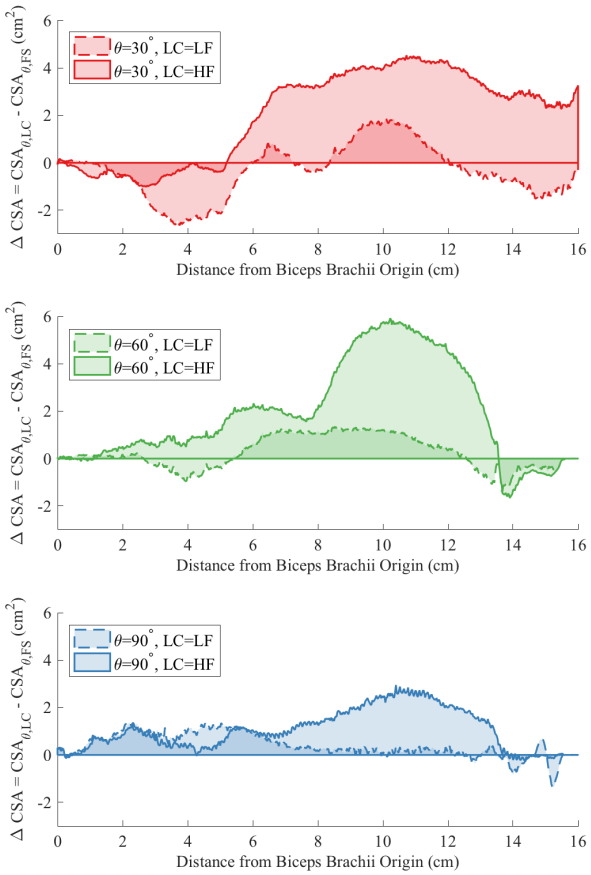

Fig. 5. Spatial variation of change in biceps brachii cross-sectional area (CSA) from that of the fully-supported volume under low (dashed) and high (solid) loading conditions. Significant variation is consistently observed in a range centered approximately 2.6cm distal from the location of maximum absolute CSA and is larger under higher loading at each configuration. These observed ΔCSA values thus indicate a candidate location from which to extract a spatially robust assistive device control signal.

B. Muscle CSA & Thickness Variation Across Loading Conditions

Figure 5 shows the spatially-varying change in muscle CSA under the two loading conditions examined, defined as the CSA under loading less the CSA while fully supported at each spatial location. The observed changes peak consistently across configurations and loading conditions at a distance of approximately 10cm from the proximal end of the muscle, roughly 63% of the way down the muscle and 2.6cm (16%) distal from the peak of the absolute maximum CSA shown in Figure 4. Over all, substantial deformation — up to 5.9cm^2, or 54% of the corresponding unloaded CSA value — is observed.

While the magnitudes of this CSA change are not comparable across configurations, as the same wrist weights induced different moments at each angle, greater changes in CSA are observed for larger loads than those of smaller loads at all angle conditions within a considerable region (8.8cm, or 55% of the total examined biceps length, roughly centered about the location of maximum CSA change, with much larger regions in the 30° and 60° cases). This suggests that an assistive device control signal could be gathered from this location and remain reasonably robust under moderate levels of sensor movement.

Although changes in muscle thickness across loading conditions were similarly defined and examined, the data proved extremely noisy, and observed signal changes were small (on the order of 0.4cm) and difficult to characterize, with no discernible peak or trend across loading conditions. This suggests that the thickness signal as defined neglects substantial muscle deformation in the unexamined dimension, and may therefore be most useful in concert with a model of muscle eccentricity, as described above. We therefore plan to undertake a more thorough study these models, and also of the most effective ways to gather a 1D muscle thickness signal (e.g., by considering different potential positions for an ultrasound sensor about the coronal plane of the arm) in future publications.

V. Conclusions, Remaining Challenges, & Future Work

The volumetric muscle data collected and examined in this study represent an excellent platform with which to verify the wide variety of existing muscle deformation models and quickly test the feasibility of new ones. At the same time, making assertions about the conceptual extensibility of the conjectures above — or even their widespread validity among individuals — will require study of a much larger subject cohort. While we plan to continue segmentation and analysis of our existing three-subject scans, substantial morphological variation across individuals makes it likely that a robust understanding of muscle deformation signals will require many more subjects of much more varied demographics.

To permit such a larger study, we are currently working to address the segmentation bottleneck — namely, the tens of hours required to segment an initial subject scan — by exploring non-rigid registration techniques to allow the mapping of one subject's muscles onto the scan of another. A large body of research relates to this registration problem as it pertains to magnetic resonance imaging (MRI); we are currently exploring ways to both apply these existing techniques to ultrasound data and to undertake similar morphological studies via MRI. As our data set grows, we are also examining ways to employ convolutional neural networks like the U-Net [26] to perform this step in a fully automated manner.

From the perspective of a prosthesis user, an ideal assistive device would allow for the independent control of force and joint angle without requiring explicit behavioral changes from the user; with this in mind, we hope to use this research framework to build a nuanced understanding of configuration- and force-related muscle deformation and the interactions between the two. Due to the complex sliding and contact dynamics involved, the configuration-related deformation signal is likely to require an especially complex model; at the same time, it may prove less necessary to

use this model explicitly during real-time device control, as a number of sensors already exist (including motion capture, electrogoniometers, and inertial measurement units) that can measure real-time kinematics. The true power of the framework we describe will be in the extraction of force-related deformation — which, given an offline model of configuration-associated deformation, may admit a clean and low-dimensional formulation, allowing for real-time, high-dimensional measurement of human dynamics.

Ultimately, the field of muscle deformation modeling could greatly benefit from its own version of the Hill model [27] — a ubiquitous, cleanly-parameterized formulation that could be applied to a wide variety of musculoskeletal modeling endeavors. While the creation of such a model will doubtless require years of rigorous system identification, both in vivo and in vitro, this paper represents a first step toward providing the type of data required for its validation, in addition to our exploration of ultrasound-based assistive device control signals.

While significant challenges remain in the translation of this work to predictive deformation models and robust control signals, we have here shown that both configuration- and force-associated muscle deformation are readily observable and can likely be used effectively in concert with other sensors to surpass existing assistive device control capabilities.

ACKNOWLEDGMENT

The authors acknowledge the aid and advice of Dr. Gregorij Kurillo, whose significant contributions to the creation of the integrated ultrasound/motion capture system, including the development of device-specific drivers and software, made data collection possible.

REFERENCES

[1] M. G. Catalano, G. Grioli, E. Farnioli, A. Serio, C. Piazza, and A. Bicchi, "Adaptive synergies for the design and control of the Pisa/IIT SoftHand," *The International Journal of Robotics Research*, vol. 33, no. 5, pp. 768–782, 2014.

[2] A. Hiraiwa, K. Shimohara, and Y. Tokunaga, "EMG pattern analysis and classification by neural network," in *1989 Proceedings of IEEE International Conference on Systems, Man and Cybernetics*, pp. 1113–1115, IEEE, 1989.

[3] E. Azizi and T. J. Roberts, "Biaxial strain and variable stiffness in aponeuroses," *The Journal of Physiology*, vol. 587, no. 17, pp. 4309–4318, 2009.

[4] S. I. Park and J. K. Hodgins, "Data-driven modeling of skin and muscle deformation," in *ACM Transactions on Graphics (TOG)*, vol. 27, p. 96, ACM, 2008.

[5] R. Lemos, M. Epstein, W. Herzog, and B. Wyvill, "Realistic skeletal muscle deformation using finite element analysis," in *2001 Proceedings of XIV Brazilian Symposium on Computer Graphics and Image Processing*, pp. 192–199, IEEE, 2001.

[6] R. R. Lemos, J. Rokne, G. V. Baranoski, Y. Kawakami, and T. Kurihara, "Modeling and simulating the deformation of human skeletal muscle based on anatomy and physiology," *Computer Animation and Virtual Worlds*, vol. 16, no. 3-4, pp. 319–330, 2005.

[7] Q.-H. Zhu, Y. Chen, and A. Kaufman, "Real-time biomechanically-based muscle volume deformation using FEM," in *Computer Graphics Forum*, vol. 17, pp. 275–284, Wiley Online Library, 1998.

[8] L. S. Krivickas, D. J. Dorer, J. Ochala, and W. R. Frontera, "Relationship between force and size in human single muscle fibres," *Experimental Physiology*, vol. 96, no. 5, pp. 539–547, 2011.

[9] J. Gulati and A. Babu, "Tonicity effects on intact single muscle fibers: relation between force and cell volume," *Science*, vol. 215, no. 4536, pp. 1109–1112, 1982.

[10] J. A. Hodgson, S.-W. Chi, J. P. Yang, J.-S. Chen, V. R. Edgerton, and S. Sinha, "Finite element modeling of passive material influence on the deformation and force output of skeletal muscle," *Journal of the Mechanical Behavior of Biomedical Materials*, vol. 9, pp. 163–183, 2012.

[11] M. Connan, E. Ruiz Ramírez, B. Vodermayer, and C. Castellini, "Assessment of a wearable force- and electromyography device and comparison of the related signals for myocontrol," *Frontiers in Neurorobotics*, vol. 10, p. 17, 2016.

[12] N. Jaquier, M. Connan, C. Castellini, and S. Calinon, "Combining electromyography and tactile myography to improve hand and wrist activity detection in prostheses," *Technologies*, vol. 5, no. 4, p. 64, 2017.

[13] N. Akhlaghi, C. A. Baker, M. Lahlou, H. Zafar, K. G. Murthy, H. S. Rangwala, J. Kosecka, W. M. Joiner, J. J. Pancrazio, and S. Sikdar, "Real-time classification of hand motions using ultrasound imaging of forearm muscles," *IEEE Transactions on Biomedical Engineering*, vol. 63, no. 8, pp. 1687–1698, 2016.

[14] P. Hodges, L. Pengel, R. Herbert, and S. Gandevia, "Measurement of muscle contraction with ultrasound imaging," *Muscle & Nerve*, vol. 27, no. 6, pp. 682–692, 2003.

[15] Y.-P. Zheng, M. Chan, J. Shi, X. Chen, and Q.-H. Huang, "Sonomyography: Monitoring morphological changes of forearm muscles in actions with the feasibility for the control of powered prosthesis," *Medical Engineering & Physics*, vol. 28, no. 5, pp. 405–415, 2006.

[16] J. McMeeken, I. Beith, D. Newham, P. Milligan, and D. Critchley, "The relationship between EMG and change in thickness of transversus abdominis," *Clinical Biomechanics*, vol. 19, no. 4, pp. 337–342, 2004.

[17] K. B. Kiesel, T. L. Uhl, F. B. Underwood, D. W. Rodd, and A. J. Nitz, "Measurement of lumbar multifidus muscle contraction with rehabilitative ultrasound imaging," *Manual Therapy*, vol. 12, no. 2, pp. 161–166, 2007.

[18] J. Shi, Y.-P. Zheng, X. Chen, and Q.-H. Huang, "Assessment of muscle fatigue using sonomyography: Muscle thickness change detected from ultrasound images," *Medical Engineering & Physics*, vol. 29, no. 4, pp. 472–479, 2007.

[19] B. M. Trindade, Y. Ono, E. D. Lemaire, and I. AlMohimeed, "Development of a wearable ultrasonic sensor and method for continuous monitoring of mechanical properties of plantar soft tissue for diabetic patients," in *2014 Proceedings of IEEE International Ultrasonics Symposium (IUS)*, pp. 2112–2115, IEEE, 2014.

[20] Y. Tsutsui, T. Tanaka, S. Kaneko, and M. Q. Feng, "Duplex ultrasonic muscle activity sensor," in *2005 Proceedings of IEEE SENSORS*, p. 4, IEEE, 2005.

[21] A. Lasso, T. Heffter, A. Rankin, C. Pinter, T. Ungi, and G. Fichtinger, "PLUS: Open-source toolkit for ultrasound-guided intervention systems," *IEEE Transactions on Biomedical Engineering*, pp. 2527–2537, Oct 2014.

[22] A. L. Tamas Ungi and G. Fichtinger, "Open-source platforms for navigated image-guided interventions," *Medical Image Analysis*, vol. 33, pp. 181–186, Oct 2016.

[23] P. A. Yushkevich, J. Piven, H. Cody Hazlett, R. Gimpel Smith, S. Ho, J. C. Gee, and G. Gerig, "User-guided 3D active contour segmentation of anatomical structures: Significantly improved efficiency and reliability," *Neuroimage*, vol. 31, no. 3, pp. 1116–1128, 2006.

[24] A. Fedorov, R. Beichel, J. Kalpathy-Cramer, J. Finet, J.-C. Fillion-Robin, S. Pujol, C. Bauer, D. Jennings, F. Fennessy, M. Sonka, J. Buatti, S. Aylward, J. V. Miller, S. Pieper, and R. Kikinis, "3D Slicer as an image computing platform for the Quantitative Imaging Network," *Magnetic Resonance Imaging*, vol. 30, pp. 1323–1341, Nov 2012.

[25] E. J. Jones, P. A. Bishop, A. K. Woods, and J. M. Green, "Cross-sectional area and muscular strength," *Sports Medicine*, vol. 38, no. 12, pp. 987–994, 2008.

[26] O. Ronneberger, P. Fischer, and T. Brox, "U-net: Convolutional networks for biomedical image segmentation," in *International Conference on Medical Image Computing and Computer-Assisted Intervention*, pp. 234–241, Springer, 2015.

[27] A. Hill, "The heat of shortening and the dynamic constants of muscle," *Proceedings of the Royal Society of London B: Biological Sciences*, vol. 126, no. 843, pp. 136–195, 1938.